COUPLED HYDRO-MECHANICAL MODELING FOR THE SLOPES IN UPPER BEAS CATCHMENT, HIMACHAL PRADESH

TARUN SINGH

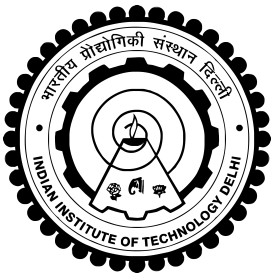

DEPARTMENT OF CIVIL ENGINEERING

INDIAN INSTITUTE OF TECHNOLOGY DELHI

AUGUST 2018

COUPLED HYDRO-MECHANICAL MODELING FOR THE SLOPES IN UPPER BEAS CATCHMENT, HIMACHAL PRADESH

by

Tarun Singh

Department of Civil Engineering

Submitted

in fulfillment of the requirements of the degree of Doctor of Philosophy

to the

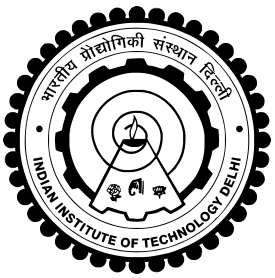

INDIAN INSTITUTE OF TECHNOLOGY DELHI

AUGUST 2018

I dedicate this thesis to my parents, ***Dr. Dayanand Singh & Late Mrs. Sumitra Singh*** *who have been a marvelous source of rationale inspiration and to my brother,* ***Ankit Singh*** *for his unconditional & absolute support. This thesis is also devoted to my guru,* ***Prof. K. S. Rao*** *who encouraged me to build my motivation towards this research.*

Certificate

This is to certify that the thesis entitled, **'Coupled Hydro-mechanical Modeling for the Slopes in Upper Beas Catchment, Himachal Pradesh'** submitted by **Mr. Tarun Singh** to the Department of Civil Engineering, Indian Institute of Technology Delhi for the award of the degree of **DOCTOR OF PHILOSOPHY** is a record of the bonafide research work carried out by him. Mr. Tarun Singh has worked under my supervision for the submission of this thesis, which to my knowledge has reached the requisite standard.

The thesis or any part of it has not been presented or submitted to any other University or Institute for any degree or diploma.

Dr. K. S. Rao

Professor

Department of Civil Engineering

Indian Institute of Technology Delhi

Hauz Khas, New Delhi 110016

Acknowledgements

I would like to express my sincere thanks to all the people who assisted me to complete this thesis. In particular, my supervisor, **Professor Kondalamahanty Seshagiri Rao** of the Indian Institute of Technology Delhi, for the guidance he offered in the course of shaping this work. You were always available for me when I needed your help. More importantly, you taught me a method of work, knowledge and critical thinking required for a research scholar. Discussion with you had always motivated me to go one step further. I also want to thank you for inviting me to multiple house lunches and dinners.

I am indebted to **Mr. Lal Mani Singh** (Executive Engineer, Border Road Organization) and **Major Parikshit Mehra** (Officer Commanding, Rohtang Tunnel) for the assistance in carrying out the landslide survey. I appreciated your patience and resilience in those rugged terrains of the Beas Kund, the Rohtang and the Dundi areas. You were a source of encouragement to the entire research team.

My special thanks go to **Mr. Ashwani Jain** (Assistance Manager, National Hydro-Power Corporation Ltd.) for your assistance in mapping landslide events in those hostile environments. I also acknowledge your assistance in AutoCAD and the digitization of survey maps.

I would like to sincerely thank **Mr. Lal Mani Singh** (Executive Engineer, Border Road Organization) for your assistance in rock sampling and field testing. The exercise required patience and perseverance. I still remember how you managed climbing the spurs of the Dundi and the Rohtang areas, with rock samples and sampling equipment on your back when most of the team members had given up.

Thanks for assisting in laboratory tests which was a long and tedious process. Through determination, the goal was timely achieved.

I am very grateful to **Major Prerit Rawat** who assisted in the social survey. This exercise required patience and understanding of the respondents. We did a good job. I wish also to thank all the respondents, including the villagers, district commissioners, and officials of the Department of Geological Survey of India and Snow & Avalanche Study Establishment (SASE). Without their cooperation, this study would not have been possible.

My colleagues in the Department of Civil Engineering at the Indian Institute of Technology Delhi and Indian Institute of Technology (Indian School of Mines) Dhanbad were very supportive and encouraging. In particular, **Mr. Awadesh Pratap Singh** (Director, Explorer Consultancy) and **Mr. Ashwani Jain** (Assistance Manager, NHPC Ltd.) who secure partial funding for multiple national and international conferences. Special thanks to **Mr. Arindom Chakraborty** (Manager, NHPC Ltd.), **Mr. Mainak Ghosh Roy** (AM, NHPC Ltd.) and **Mr. Kundu** (Director, Explore) for the moral support and encouragement.

I appreciate the patience, support and encouragement of **Mr. Ankit Singh** and a special thanks for translating the abstract and keywords into hindi; God bless you abundantly.

I am very grateful to **Council of Scientific & Industrial Research (CSIR)**, Department of Science and Technology, Government of India for providing research funds, scholarship, and fund for meeting some of the living and traveling expenses during the study period.

My very special thanks go to the "great" driver **Mr Raju Mondal**. Despite

being sick in the course of the study you forged ahead till the last day. You proved tous all that determination and commitment are great virtues. To the porters both in Kullu and Lahaul & Spiti Districts, I appreciated your support. You led us to where landslides occurred.

To friends, thanks for the moral support and encouragement. Special appreciation to **Mr Ankit Singh**, Centre of Studies in Resources Engineering at the Indian Institute of Technology Bombay for proof-reading the initial drafts.

To **Mr. Darwan Singh Gussain** (Retd.) and **Mr. Alok Kumar** (Rock Mechanics Laboratory), **Mr. Debyendu Biswas** (Engineering Geology Laboratory) and **Mr. Manoj Kumar Neelam** (Soil Mechanics Laboratory), for the technical support rendered anytime. Your talent is greatly appreciated.

Finally, untold love and thanks go to **Aditya, Rebecca, Endalu, Prateek, Ankesh, Swapnil, Gopi, Chandan, Krishnamurty, Mahin, Falaq** and other Geotechnical Research Group (GRG) Members who in their unique ways have made this work possible.

Tarun Singh

Abstract

A landslide is a downslope movement of the rock mass, soil, debris or any mixture of these materials, of the sloping surface under the influence of the gravity. In mountainous regions, landslides are the most frequent natural hazards, causing tremendous loss of life, economy, property and creating a vast disturbance in the livelihood of the people. Complex geology and weak geological structures, rugged and steep terrain, high relief variations along with seasonal monsoon rainfall give rise to a high degree of fragility and instability in the whole mountain system. Thus, the detailed studies for material behavior, slope kinematics, rainfall frequency, assessment of landslide hazards and numerical modeling is of utmost importance to understand their behavior, deformation mechanisms leading to failure in varying conditions of stability.

It is well-known that water is one of the major triggers of landslides. Numerous landslide studies discuss different effects that water may have on slope stability: decreasing suction, rising groundwater table and subsequent increasing of pore water pressure, groundwater exfiltration from the bedrock, seepage erosion, hydraulic uplift pressure from below the landslide, and influence of water on the plasticity of the landslide. The first objective of this study is to investigate the dominating controlling parameter for the landslide in UBC and to access the origin, flow paths and effect of rainfall in ten different slopes and landslides in UBC.

The geotechnical parameters e.g. physical and mechanical properties play a very important role in a precise forecast of rock behavior under such inconsistent conditions. The mechanical properties of rocks change with density, porosity, a

variation of mineral assemblage, grain size and texture and effective pressures acting on them. A comprehensive study has been undertaken using three varieties of rocks obtained from the UBC in the Himalayan region. Attention has been paid to their petrographic and petrofabric analyses through Scanning Electron Microscope (SEM) and thin sections studies. Uniaxial compressive strength, Brazilian tensile strength and triaxial strength tests are conducted on three different rock samples namely Phyllitic-quartzite (PQ), Quarzitic-phyllite (QP) and Migmatitic-gneiss (MG) to understand the nature of failure patterns. Strength and deformation behavior of the rocks in both dry and saturated conditions are also defined and compared with various properties. Laboratory testing of the collected samples has been performed using ISRM (2007-14) suggested methods of rock characterization to evaluate shear strength parameters.

For the assessment of the natural stability of rock slopes, kinematic analysis technique is extensively used. This technique makes use of dominant discontinuity planes within slope mass to forecast the probability of sliding, wedging and falling. As rock slope surface is either concave or convex shaped, its changing strike also plays a significant role in the kinematic analysis. These slopes will have two or more planar surfaces and are termed as multi-faced slopes (MFS). The details of kinematic analysis performed on these MFS and gives the stability index for these slopes with the change in strike direction. Three cases are used for the further analysis. Case 1 (Planar sliding), when the failure is based on only one joint set and is planar in nature. Case 2 (Double plane sliding / Wedging), when wedge block is formed and sliding is along both planes, formed by either, the intersection of dominant joint sets or by two slope surfaces. Case 3 (Toppling), when the block topples, either showing flexural toppling or direct toppling. Results of the cases study are presented.

The information regarding long-term trends, variability, extreme events etc. of the rainfall over a catchment are accessed through Indian Meteorological Data. For the accurate prediction of rainfall diurnal and spatial variation, and amount of rainfall at the slightest scale, a new high resolution gridded rainfall database is created. This database is used to study the orogenic effect on rainfall and to predict the 10, 20, 50 and 100-year rainfall return period. Isohyet maps are created at monthly and annual scale for 113 years (1901-2013) representing variability over UBC.

For determining the susceptible areas to slope failure, a multiparametric landslide hazard zonation is performed in ArcGIS Environment at the catchment scale. The effect of rainfall in changing the percentage of area under a particular hazard (very low to the extreme) is determined by overlying the isohyet maps for rainfall return period with the developed LHZ maps. This new approach of wet LHZ is compared with available landslide inventory, which shows high correlation factor over dry LHZ.

Preferential flow paths, such as cracks, macropores, fissures, pipes etc. are common features of heterogeneous slopes. During intense rainstorms, the preferential flow has a significant influence on subsurface flow and slope stability. Dual-permeability models are widely used to simulate preferential flow but have not been incorporated into hydro-mechanical models. In this study, the COMSOL Multiphysics software is used to couple a dual-permeability model with a mechanics model for landslide stability evaluation. Detailed information is provided on how to incorporate current hydrological and mechanics theories into COMSOL. A total of ten slopes are modeled in 3D and variation of the factor of safety, pore water pressure, the degree of saturation and deformation over the course of 113 years is recorded. The results are further analyzed to elucidate the implications of rainfall data for determining and predicting the arising instability within slope masses.

सारांश:

एक भूस्खलन गुरुत्वाकर्ष्रण के प्रभाव के कारण, ढलान की सतह परं मौजूद, चट्टान पिंड, मिट्टी, मलबे या इन सामग्रियों के मिश्रण का एक डाउनस्लोप संचलन है। पहाड़ी क्षेत्रों में, भूस्खलन सबसे नित्य प्राकृतिक विपत्ति है, जिससे लोगों के जीवन की भारी मात्रा में क्षति, अर्थ्व्यवस्था, संपत्ति और आजीविका में व्यापक परेशानी पैदा हो रही है। जटिल भूविज्ञान और कमजोर भौगोलिक संरचनाएं, विषम और खड़ी इलाके, मौसमी मानसून र्व्षा के साथ उच्च भूभाग विविधता पूरे पहाड़ी व्यवस्था में उच्च स्तर की कमजोरी और अस्थिरता को जन्म देती है। इस प्रकार, भौतिक व्यवहार, असम भूमि कीनेमेटीक्स, बारिश आवृत्ति, भूस्खलन संबंधी खतरों का आकलन और संख्यात्मक मॉडलिंग का विस्तृत अध्ययन उनके व्यवहार, विरूपण तंत्र को समझने के लिए बेहद महत्वर्पूण है, जिससे स्थिरता की स्थिति अलग-अलग अवस्था में विफल हो सकती है।

यह अच्छी तरह से ज्ञात है कि पानी भूस्खलन के प्रमुख ट्रिग्स में से एक है। अनेक भूस्खलन अध्ययन पानी के, ढलान स्थिरता पर अलग-अलग प्रभावों की र्च्चा करते हैं : घटता हुआ चुसाव, भूजल की बढ़ती तालिका और उत्तरर्व्ती रंध्र जल दाब की वृद्धि, बेड रॉक से भूजल एक्सफ़िल्टरेशन, भूजल का क्षरण, भूस्खलन के नीचे से हाइड्रोलिक उत्थान का दबाव और भूस्खलन की सुनम्यता पर पानी का प्रभाव। इस अध्ययन का पहला उद्देश्य यूबीसी में भूस्खलन के लिए प्रभुत्व नियंत्रण पैरामीटर की जांच करना है और यूबीसी में दस अलग-अलग ढलानों और भूस्खलन का उद्गम, प्रवाह पथ और र्व्षा के प्रभाव का अभिगम करना है।

भू-तकनीकी पैरामीटर उदाहरर्णाथ भौतिक और यांत्रिक गुण, ऐसी विसंगत परिस्थितियों में रॉक व्यवहार के सटीक पूर्वानुमान में महत्वर्पूण भूमिका निभाते हैं। चट्टानों के यांत्रिक गुण जैसे घनत्व, छिद्रपूर्ण्ता, खनिज संयोजन, कण आकार और बनावट उन पर प्रभावी दबावों के साथ परिवर्त्ति हो जाते हैं। हिमालयी क्षेत्र में यूबीसी से प्राप्त तीन प्रकार की चट्टानों का एक व्यापक अध्ययन किया गया है। स्कैनिंग इलेक्ट्रॉन माइक्रोस्कोप (एसईएम) और पतली धाराओं के अध्ययन

के माध्यम से उनके पेट्रोग्राफिक और पेट्रोफैब्रिक विश्लेषण पर ध्यान दिया गया है। यूनिअक्सियल कॉम्प्रेसिव शक्ति, ब्राज़ीलियाई तन्यता शक्ति और त्रिकोणीय शक्ति परीक्षण तीन अलग रॉक नमूनों अर्थात्: फाइलिटिक-क्वार्ट्जाइट (पीक्यू), क्वार्ज़्िटिक-फायलाइन (क्यूपि) और मिगमैटिक-गनीस (एमजी) के विफलता पैर्ट्न की प्रकृति को समझने के लिए संचालित किये गए हैं। एकत्रित नमूनों का प्रयोगशाला परीक्षण, आई.अस.आर.एँम (2007-14) द्वारा सुझाए गए रॉक विशेषीकरण के तरीको का उपयोग कर अपरूपण शक्ति पैरामीटर का मूल्यांकन के लिए किया गया है।

चट्टान की ढलानों की प्राकृतिक स्थिरता के मूल्यांकन के लिए, किनेमेटिक विश्लेषण तकनीक का उपयोग बड़े पैमाने पर किया जाता है। यह तकनीक ढलान के भीतर प्रमुख असंतुलन सतह का इस्तेमाल करता है ताकि फिसलने, पच्चीकारी और गिरने की संभावना का अनुमान लगाया जा सके। चूंकि रॉक ढलान की सतह या तो अवतल या उत्तल आकार होती है, इसकी बदलती स्ट्राइक भी काइनेमैटिक विश्लेषण में महत्वर्पूण भूमिका निभाती है। इन ढलानों में दो या अधिक प्लुलानर सतहें होंगी और उन्हें बहु-सामना वाली ढलान (एमएफएस) कहा जाता है। इन एमएफएस पर स्ट्राइक की दिशा में परिवर्त्न के साथ किए गए काइनेमैटिक विश्लेषण का ब्योरा इन ढलानों के लिए स्थिरता सूचकांक देता है। आगे के विश्लेषण के लिए तीन अवस्थाओं का उपयोग किया गया है। प्रकरण प्रथम (प्लुलानर फिसलने), जब विफलता केवल एक संयुक्त सेट पर आधारित और स्वभाव में प्लुलानर होती है। प्रकरण द्वितीय (डबल स्लिस स्लाइडिंग / वेजिंग), जब पच्चर ब्लुलॉक का गठन होता है और सरकन दोनों सतह के साथ होती है, जो की, प्रमुख संयुक्त सेट के प्रतिच्छेदन अन्यतर दो ढलान सतहों द्वारा निर्म्ित होता है। प्रकरण तृतीय (टोपलिंग), जब ब्लुलॉक गिर पड़ता है, या तो, फ्लेक्झल टोपलिंग या सीधी टोपलिंग दर्शाते हुए। प्रकरण के अध्ययन के परिणाम प्रस्तुत किए गए हैं।

जलग्रह में र्वषा के दौरान लंबे दीर्घार्वधि प्रवृत्तियों, परिवर्त्नशीलता, चरम घटनाओं आदि के बारे में जानकारी भारतीय मौसम संबंधी डेटा द्वारा अभिगम कि गयी हैं। बारिश कि दैनिक और

स्थानिक भिन्नता की सटीक भविष्यवाणी के लिए और अल्प स्तर पर बारिश कि मात्रा के मान के लिए एक नया उच्च रेसोलुशन वर्षा डेटाबेस बनाया गया है। इस डेटाबेस का उपयोग वर्षा के ओरोजेनिक प्रभाव का अध्ययन करने के लिए किया गया है और 10, 20, 50 और 100-वर्षीय बारिश अवधि की भविष्यवाणी करने के लिए किया गया है। यूबीसी पर इसोहइत नक्शे 113 वर्ष (1901-2013) की परिवर्तिता दर्शाने के लिए मासिक और वार्षिक पैमाने पर बनाये गए है।

असम भूमि की विफलता के लिए अतिसंवेदनशील क्षेत्रों का निर्धारण करने के लिए, एक मल्टीपैमेट्रिक भूस्खलन जोखिम क्षेत्र का निष्पादन आर्कजीआईअस परिवेश में कैचमेंट स्केल पर किया गया है। किसी विशेष खतरा (बहुत चरम से कम) के तहत क्षेत्र के प्रतिशत को बदलने में बारिश का प्रभाव, विकसित ल.अच्.जेड. मैप्स के साथ बारिश की अवधि के लिए इसोहइत नक्शे के आधार पर निर्धारित किया गया है। नम एलएचझेड के इस नए दृष्टिकोण की तुलना भूस्खलन की उपलब्ध सूची से की गयी है, जो सूखी एलएचझेड पर उच्च सहसंबंध कारक दर्शाती है।

अधिमान्य प्रवाह पथ, जैसे कि दरारें, मैक्रोर्प्रोस, फिर्श्स, पाइप आदि विषम ढलानों की सामान्य विशेषताएं हैं। तीव्र बारिश के दौरान, तरजीही प्रवाह का प्रभाव उपसतह प्रवाह और असम भूमि की स्थिरता पर महत्वर्पूण प्रभाव डालता है। दोहरे पारगम्यता मॉडल को व्यापक रूप से तरजीही प्रवाह अनुकरण के लिए उपयोग किया जाता है लेकिन जल-यांत्रिक मॉडलों में शामिल नहीं किया गया है। इस अध्ययन में, कॉसमोल मल्टीफेहिक्स सॉफ्टवेयर को द्वि-पारगम्यता मॉडल को यांत्रिकी मॉडल के साथ भूस्खलन स्थिरता मूल्यांकन के लिए संयोजित किया गया है। कॉमएसओएल में वर्तमान हाइड्रोलॉजिकल और मैकेनिकल सिद्धांतों को शामिल करने के बारे में विस्तृत जानकारी दी गई है। कुल दस ढलानों को त्रिविम दृश्यन में तैयार किया गया है और सुरक्षा के कारक के विविधता, उत्तरवर्ती रंध्र जल दाब, संतृप्ति की मात्रा और विकृति 113 वर्ष के दौरान अभिलिखित की गई है। ढलान के भीतर अस्थिरता को निर्धारित करने और अनुमान लगाने के लिए और वर्षा डेटा के निहितार्थ को स्पष्ट करने के परिणामों का आगे विश्लेषण किया गया है।

Contents

Certificate i

Acknowledgements iii

Abstract vii

Abstract (Hindi) xi

Contents xv

List of Figures xxv

List of Tables xli

List of Abbreviations xlvii

List of Notations li

1 Introduction 1

1.1 General 1

1.2 Limitations and Gap Area 5

1.3 Scope and Objectives of the Thesis 7

1.4 Methodology 10

1.5 Organization of the Thesis 11

2 Literature Review 17

2.1 Overview 17

2.1.1 Slope Failure Classification 19

2.1.2 Factors Affecting Slope Failure 20

2.2 Slope Failure Mechanisms 25
2.2.1 Modes of Failure 25
2.2.1.1 Planar failure 26
2.2.1.2 Wedge failure 29
2.2.1.3 Toppling failure 29
2.2.1.4 Rotational/Circular failure 30
2.3 Continuous Slope Mass Rating 30
2.4 Kinematic Analysis 33
2.4.1 Stereonet-based Kinematic Analysis 35
2.4.2 Probabilistic Method 37
2.5 Mechanical Properties of Slope Material 38
2.6 Hydrological Properties of Slope Material 40
2.7 Landslide Hazard Analysis 43
2.7.1 Introduction 43
2.7.1.1 Natural Hazard 44
2.7.1.2 Vulnerability 44
2.7.1.3 Risk 45
2.7.1.4 Element at Risk 45
2.7.1.5 Total Risk 45
2.7.2 Hazard Evaluation Factors 47
2.7.3 Method of Landslide Hazard Analysis 48
2.7.4 Uses of Landslide Hazard Analysis 49
2.7.5 Assumptions in Landslide Hazard Analysis 50
2.8 Pore Water Pressure and Effect 51
2.8.1 Influence of Moisture on the Strength of Rocks 51
2.8.1.1 Pore water pressure in tension crack 55

2.8.2 PWP due to Isotropic Stress Application 56
2.8.3 Conceptual Models for Preferential Flow Path 58
2.8.3.1 Dual permeability model 58
2.8.3.2 Single porosity models 61
2.8.4 Rainfall Infiltration Theory 61
2.8.5 Wetting Front and Moisture Redistribution 65
2.8.6 Shear Strength of Unsaturated Material 66
2.8.7 Catchment-scale Models for Rainfall Induced Landslide 69
2.9 Discussion 72

3 Field Investigation 75
3.1 Introduction 75
3.2 Location and Accessibility 76
3.3 Reconnaissance Survey 82
3.4 Geology 87
3.4.1 Stratigraphic Sequence 87
3.4.2 Metamorphism 90
3.4.2.1 Manikaran quartzite 90
3.4.2.2 Jutogh formation 90
3.4.2.3 Khamrada formation 92
3.4.2.4 Vaikrita group 92
3.4.3 Metamorphic Inversion 93
3.5 Structures 93
3.5.1 Recumbent Folding 93
3.5.2 Cross Folding 94
3.5.3 Flexure Folding 95

3.6 Geomorphology 95
3.6.1 Geomorphology of Beas River Valley 96
3.6.1.1 Geomorphology of Solang valley 96
3.6.1.2 Beas valley 99
3.6.2 Drainage 101
3.6.3 Relief 104
3.6.4 Slope 106
3.6.5 Soil 106
3.6.6 Land Uses and Land Cover 108
3.6.7 Climate 110
3.7 Geotechnical Survey 116
3.7.1 Landslide Locations and Distribution 116
3.7.2 Slope Characterization 125
3.7.3 Joint Mapping 127
3.8 Field Tests 130
3.8.1 Tilt Test 130
3.8.2 Schmidt Rebound Test 131
3.9 Discussion 134

4 Laboratory Study 137
4.1 Introduction 137
4.2 Description of Rocks 137
4.3 Petrological Studies 139
4.3.1 Thin Section Studies 140
4.3.1.1 Phyllitic-quartzite 140
4.3.1.2 Quartzitic-phyllite 141

4.3.1.3 Migmatitic-gneiss 142
4.3.2 X-ray Powder Diffraction 144
4.3.3 Scanning Electron Microscopy 147
4.4 Physico-mechanical Properties of Rocks 154
4.4.1 Sample Preparation 155
4.4.2 Unit Weight, Density and Porosity 156
4.4.3 Specific Gravity 157
4.4.4 Slake Durability Index 158
4.4.5 Indirect Tensile (Brazilian) Strength 159
4.4.6 Uniaxial Compressive Strength 162
4.4.6.1 Modulus of elasticity and Poisson's ratio 163
4.4.6.2 Effect of saturation 165
4.4.6.3 Deere-Miller classification 166
4.4.7 Triaxial Compressive Strength 167
4.4.7.1 Effect of saturation 169
4.4.8 Failure Pattern 171
4.4.9 Oblique Shear Testing 173
4.4.10 Permeability 175
4.4.10.1 Rock permeability and effect of confining pressure 176
4.5 Discussions 180

5 Kinematic Analysis 183

5.1 Introduction 183
5.1.1 Selected Landslides and Locations 184
5.2 Joint Data Statistical Analysis 185
5.3 Kinematic Analysis 188

5.4 Slope Response Analysis 192

5.5 Discussion 205

6 Rainfall Analysis 219

6.1 Introduction 219

6.2 Gridded Daily Rainfall Data 220

6.2.1 Available Data 220

6.2.2 Data Used 221

6.2.3 Creation of High Resolution Gridded Rainfall Data 222

6.2.4 Results 223

6.2.5 Discussion 227

6.3 Generation of Isohyets Maps (Catchment Scale) 230

6.4 Rainfall Analysis for Selected Slopes 250

6.4.1 Mean Monthly Average 250

6.4.2 Annual Rainfall Trends 256

6.5 Return Period and Frequency Analysis for Rainfall 257

6.5.1 Comparison of Distribution Method 257

6.5.2 Gumbel Distribution (GEV Type-I) 265

6.5.3 Return Period 272

6.6 Discussions 273

7 Rainfall Based Landslide Hazard Zonation 275

7.1 Introduction 275

7.2 Datasets and Sources 276

7.3 Predisposing Parameters of Landslide Hazard 278

7.3.1 Slope Angle 280

7.3.2 Slope Aspect 280

7.3.3 Relative Relief of Surface 284
7.3.4 Land Use and Land Cover 286
7.3.5 Geological Setup 287
7.3.6 Seismo Tectonics 289
7.3.7 Proximity to Faults 292
7.3.8 Proximity to Roads 294
7.3.9 Drainage Buffer and Drainage Density 296
7.4 Selection of Optimal Parameters 300
7.5 Pre-processing Dataset and GIS Data 303
7.5.1 Phase I 303
7.5.2 Phase II 304
7.5.3 Phase III 304
7.5.4 Phase IV 306
7.6 Data Integration and Landslide Hazard Analysis 307
7.7 Integrated Rainfall Analysis 313
7.7.1 Effect of Rainfall on Slopes 320
7.7.2 Rainfall Integrated Landslide Hazard Zonation 320
7.8 Assessment and Discussion 327

8 Coupled Hydro-mechanical Modeling and Numerical Analysis 329
8.1 Introduction 329
8.2 Numerical Simulation 331
8.2.1 Numerical Model 332
8.2.2 Study Definitions 332
8.2.3 Mesh Generation 337
8.2.4 Boundary Condition 338

8.2.5 Initial Conditions 339
8.2.6 Model Properties 340
8.3 Sensitivity Analysis 345
8.3.1 Variation of Factor of Safety with Rainfall 345
8.3.2 Variation of Pore Water Pressure with Rainfall 352
8.3.3 Cumulative Total Displacement Generated by Rainfall 359
8.3.4 Variation of Degree of Saturation with Rainfall 366
8.4 Discussion 372

9 Summary, Conclusions and Future Work 375
9.1 General 375
9.2 Conclusions 376
9.2.1 Field Investigation 377
9.2.2 Laboratory Analysis and Experimentation 378
9.2.3 Kinematic Analysis 379
9.2.4 Rainfall Analysis 380
9.2.5 Landslide Hazard Zonation 381
9.2.6 Coupled Hydro-Mechanical Modeling 382
9.3 Significance of Present Study 383
9.4 Limitations of the Work 384
9.5 Future Aspects 385

References 387

A Landslide History 411

B Records and Raw Site Data 425

C Kinematic Analysis Data 477

D Numerical Modeling Data **511**

D.1 Richard's Model 511

D.2 Solid Mechanics Model 512

E Other Recorded Landslides in UBC **553**

Vitae **559**

F.1 Publications and Talks 560

F.1.1 Papers in Refereed Journals 560

F.1.2 Papers Presented in International Conferences 560

F.1.3 Papers in other Conferences 561

List of Figures

1.1 Comparison of Landslide Casualties across World and India 2

1.2 Prevailing Landslide Causing Factors in Himalayas and their Percentages 3

1.3 Some Consequences of the Landslide in the Himalayas, Affected Peoples, Buried Bodies and Property Loss. 4

1.4 Mind Map for Objective (i.) 8

1.5 Mind Map for Objective (ii.) 8

1.6 Mind Map for Objective (iii.) 8

1.7 Mind Map for Objective (iv.) 9

1.8 Mind Map for Objective (v.) 9

1.9 Mind Map for Objective (vi.) 9

1.10 Algorithm for Adopted Methodology 12

2.1 Varnes Landslide Classifications Scheme Represented in Pictures 22

2.2 Stress Vectors Within a Slope (Rose and Hungr, 2007) for Pre and Post Failure of Active and Reactivated Landslide 23

2.3 Stress Vectors Within a Slope (Dietrich et al., 2003) 26

2.4 Three Levels of Stability Analysis and Related Failure Mechanisms (Stead et al., 2006) 27

2.5 Three Types of Rock Slope Failures (Hoek and Bray, 1981a) 28

2.6 Circular Failure Mode (Hoek and Bray, 1981a) for Highly Jointed Rock Masses 31

2.7 Mohr Rupture Envelopes Outlining the Effect of Moisture on the UCS of Quartzite. (Reconstructed from Colback and Wiid (1965)) 52

2.8 Mohr Circles of Total Stress and Effective Stress 53

2.9 Definition of Effective Stress (Terzaghi, 1925) 53

2.10 Total Normal Stresses Model for Slope Mass 54

2.11 Effect of Water Pressure in a Tension Crack (Here: $y = \psi$) 55

2.12 Rock Block under Isotropic Stress Application and Resulting Changes 57

2.13 Definition of C_c: Volume Change Due to Compression with Zero Excess PWP (Note: V is the Volume of the Rock Element at any Given Value of σ') 57

2.14 Dual-permeability Models: (a) Horizontal Fractures and Matrix Blocks, (b) Spherical Matrix Blocks, and (c) Cubical Matrix Blocks 59

2.15 Water Retention Curve (WRC) with Approximate Locations of Saturated Water Content (θ_s) , Residual Water Content (θ_r) , Air-Entry Value $(u_a - u_w)_r$ (Zhan and Ng, 2004) 63

2.16 Wetting Front Development in the Heber Green and Ampt (1911) Model 66

2.17 3D Failure Envelope for Unsaturated Material 68

2.18 Sketch of an Elementary Drainage Area: (Top) Planar View and (Bottom) Longitudinal Section 70

3.1 Images of Few Reported Landslide in Upper Beas Catchment (Collage 1; Source: Open Media) 77

3.2 Images of Few Reported Landslide in Upper Beas Catchment (Collage 2; Source: Open Media) 78

3.3 Mosaiced Toposheet Map of the Upper Beas Catchment 80

3.4 Road Map of the Upper Beas Catchment 81

3.5 Google Earth Imagery for Upper Beas Catchment 84

3.6 Digital Elevation Model (3D) for the Upper Beas Catchment 85

3.7 False Color Composite (FCC) Imagery for the Upper Beas Catchment 86

3.8 Major Lithological and Geological Groups of the Upper Beas Catchment 88

3.9 Drainage Map for the Upper Beas Catchment 102

3.10 Relief Map for the Upper Beas Catchment 105

3.11 Slope Map for the Upper Beas Catchment 107

3.12 Soil Map of the Upper Beas Catchment 109

3.13 Land Use and Land Cover Map for Upper Beas Catchment 111

3.14 Last 100 Year (1915-2016) Monthly Maximum Rainfall for Kullu IMD Station and Average for 100 Years 113

3.15 Last 100 Year (1915-2016) Monthly Maximum Rainfall for Lahaul & Spiti IMD Station and Average for 100 Years 113

3.16 Last 100 Year (1915-2016) Average of Monthly Minimum, Average and Maximum Temperature (in ^oC) for Kullu and Lahaul & Spiti IMD Station 115

3.17 Landslide Inventory Map showing Landslides History (1978 -2010), Events (2011 - 2016) and Few Remotely Identified Landslides 118

3.18 Location of Major Landslides and Landslide Zone Identified within Upper Beas Catchment 119

3.19 Slope SA/1 121

3.20 Slope SA/1 121

3.21 Slope SA/3 121

3.22 Slope SA/4 121

3.23 Slope SA/5 122

3.24 Slope SA/6 122

3.25 Slope SA/7 123

3.26 Slope SA/8 123

3.27 Slope SA/9 124

3.28 Slope SA/10 124

3.29 3D Model Showing Methodology of Tilt Test 131

3.30 Sliding Angle of Rock Joint Obtained using Tilt Tests conduced for Dry and Saturated Samples (L1-L22) 132

3.31 Schmidt Hammer and its Scale (zoomed) 133

3.32 Correlation Chart for L-type Schmidt Hammer 133

3.33 Schmidt Rebound Values for Joints under Dry and Saturated Condition (L1 - L22) 133

4.1 Flowchart for the Experimental Program 138

4.2 Thin Section Imagery for Phyllitic-quartzite under Plane-polarized (Above) and Cross-Polarized (Below) Light 141

4.3 Thin Section Imagery for Quartzitic-phyllite under a Plane-polarized (Above) and Cross-Polarized (Below) Light 142

4.4 Thin Section Imagery for Migmatitic-gneiss under a Plane-polarized (Above) and Cross-Polarized (Below) Light 143

4.5 Rigaku MiniFlex 600 X-ray Diffractometer 145

4.6 X-ray Powder Diffraction Pattern Correction, Peak Identification and Miller Indices 145

4.7 X-ray Powder Diffraction Pattern and Phase Identification using Dominant Peak Obtained for Rock Powdered Specimen 1-3 (Top to Bottom) 146

4.8 Carl Zeiss EVO-18 Scanning Electron Microscope 148

4.9 Scanning Electron Microscope Images for Phyllitic-quartzite 150

4.10 Scanning Electron Microscope Images for Quartzitic-phyllite 151

4.11 Scanning Electron Microscope Images for Migmatitic-gneiss 152

4.12 Flowchart for the Physico-mechanical Experimentation Program 156

4.13 Porosity of Phyllitic-quartzite, Quartzitic-phyllite and Migmatitic-gneiss 158

4.14 Brazilian Tensile Strength (σ_t) Values at Various Inclination Angle (β) Angle under Dry and Saturated Condition 161

4.15 Uniaxial Compression Strength Testing Machine with Automatic Data-recorder Connected to Computer 163

4.16 Stress-Strain Plot for Phyllitic-quartzite under Uniaxial Compression Strength Testing 164

4.17 Stress-Strain Plot for Quartzitic-phyllite under Uniaxial Compression Strength Testing 164

4.18 Stress-Strain Plot for Migmatitic-gneiss under Uniaxial Compression Strength Testing 165

4.19 Deere and Miller (1966) Classification of Intact Rock 166

4.20 Triaxial Testing Machine with Confining Pressure Unit and Triaxial Cell 168

4.21 Strength Envelopes for Phyllitic-quartzite, Quartzitic-phyllite and Migmatitic-gneiss 169

4.22 Mohr's Circles for Phyllitic-quartzite, Quartzitic-phyllite and Migmatitic-gneiss under Dry and Saturated Condition 170

4.23 p-q Plot for Phyllitic-quartzite, Quartzitic-phyllite and Migmatitic-gneiss Rock Specimens under Dry and Saturated Condition 172

4.24 IIT Delhi (Rao, 1984) Failure Criterion for Phyllitic-quartzite, Quartzitic-phyllite and Migmatitic-gneiss Rock Specimens under Dry and Saturated Condition 173

4.25 Failure Patterns Obtained under Uniaxial Compression Strength Testing 174

4.26 Failure Patterns Obtained under Triaxial Compression Strength Testing 175

4.27 Shear Stress vs. Normal Stress Plot for Phyllitic-quartzite, Quartzitic-phyllite and Migmatitic-gneiss Rock Specimens under Dry and Saturated Condition. 176

4.28 Permeability Apparatus with Confining Pressure Unit 177

4.29 Permeability vs. Pressure Plot for Phyllitic-quartzite Rock Specimens. 178

4.30 Permeability vs. Pressure Plot for Quartzitic-phyllite Rock Specimens. 178

4.31 Permeability vs. Pressure Plot for Migmatitic-gneiss Rock Specimens. 179

4.32 Comparison of Permeability for Phyllitic-quartzite, Quartzitic-phyllite and Migmatitic-gneiss Rock Specimens under Different Pressures. 179

5.1 Rose Diagrams for Slope SA/1 to SA/6 187

5.2 Rose Diagrams for Slope SA/7 to SA/10 188

5.3 Discontinuities Data Cluster Analysis for Slope SA/1 to SA/6 189

5.4 Discontinuities Data Cluster Analysis for Slope SA/7 to SA/10 190

5.5 Algorithm for Kinematic Analysis 192

5.6 Stereographic Plots of Kinematic Analysis for (a) Planar Sliding, (b) Wedge Sliding, (c) Flexural Toppling and (d) Direct Toppling under Dry and Saturated Conditions (Slope Code-SA/1) 193

5.7 Stereographic Plots of Kinematic Analysis for (a) Planar Sliding, (b) Wedge Sliding, (c) Flexural Toppling and (d) Direct Toppling under Dry and Saturated Conditions (Slope Code-SA/2) 194

5.8 Stereographic Plots of Kinematic Analysis for (a) Planar Sliding, (b) Wedge Sliding, (c) Flexural Toppling and (d) Direct Toppling under Dry and Saturated Conditions (Slope Code-SA/3) 195

5.9 Stereographic Plots of Kinematic Analysis for (a) Planar Sliding, (b) Wedge Sliding, (c) Flexural Toppling and (d) Direct Toppling under Dry and Saturated Conditions (Slope Code-SA/4) 196

5.10 Stereographic Plots of Kinematic Analysis for (a) Planar Sliding, (b) Wedge Sliding, (c) Flexural Toppling and (d) Direct Toppling under Dry and Saturated Conditions (Slope Code-SA/5) 197

5.11 Stereographic Plots of Kinematic Analysis for (a) Planar Sliding, (b) Wedge Sliding, (c) Flexural Toppling and (d) Direct Toppling under Dry and Saturated Conditions (Slope Code-SA/6) 198

5.12 Stereographic Plots of Kinematic Analysis for (a) Planar Sliding, (b) Wedge Sliding, (c) Flexural Toppling and (d) Direct Toppling under Dry and Saturated Conditions (Slope Code-SA/7) 199

5.13 Stereographic Plots of Kinematic Analysis for (a) Planar Sliding, (b) Wedge Sliding, (c) Flexural Toppling and (d) Direct Toppling under Dry and Saturated Conditions (Slope Code-SA/8) 200

5.14 Stereographic Plots of Kinematic Analysis for (a) Planar Sliding, (b) Wedge Sliding, (c) Flexural Toppling and (d) Direct Toppling under Dry and Saturated Conditions (Slope Code-SA/9) 201

5.15 Stereographic Plots of Kinematic Analysis for (a) Planar Sliding, (b) Wedge Sliding, (c) Flexural Toppling and (d) Direct Toppling under Dry and Saturated Conditions (Slope Code-SA/10) 202

5.16 Graphs Showing Variation in Critical Percentage of Failure under (a) Planar Sliding, (b) Wedge Sliding and (c) Flexural Toppling for Change in Slope Dip Angle (Slope Code-SA1) 206

5.17 Graphs Showing Variation in Critical Percentage of Failure under (a) Planar Sliding, (b) Wedge Sliding and (c) Flexural Toppling for Change in Slope Dip Direction (Slope Code-SA1) 206

5.18 Graphs Showing Variation in Critical Percentage of Failure under (a) Planar Sliding, (b) Wedge Sliding and (c) Flexural Toppling for Change in Slope Dip Angle (Slope Code-SA2) 207

5.19 Graphs Showing Variation in Critical Percentage of Failure under (a) Planar Sliding, (b) Wedge Sliding and (c) Flexural Toppling for Change in Slope Dip Direction (Slope Code-SA2) 207

5.20 Graphs Showing Variation in Critical Percentage of Failure under (a) Planar Sliding, (b) Wedge Sliding and (c) Flexural Toppling for Change in Slope Dip Angle (Slope Code-SA3) 208

5.21 Graphs Showing Variation in Critical Percentage of Failure under (a) Planar Sliding, (b) Wedge Sliding and (c) Flexural Toppling for Change in Slope Dip Direction (Slope Code-SA3) 208

5.22 Graphs Showing Variation in Critical Percentage of Failure under (a) Planar Sliding, (b) Wedge Sliding and (c) Flexural Toppling for Change in Slope Dip Angle (Slope Code-SA4) 209

5.23 Graphs Showing Variation in Critical Percentage of Failure under (a) Planar Sliding, (b) Wedge Sliding and (c) Flexural Toppling for Change in Slope Dip Direction (Slope Code-SA4) 209

5.24 Graphs Showing Variation in Critical Percentage of Failure under (a) Planar Sliding, (b) Wedge Sliding and (c) Flexural Toppling for Change in Slope Dip Angle (Slope Code-SA5) 210

5.25 Graphs Showing Variation in Critical Percentage of Failure under (a) Planar Sliding, (b) Wedge Sliding and (c) Flexural Toppling for Change in Slope Dip Direction (Slope Code-SA5) 210

5.26 Graphs Showing Variation in Critical Percentage of Failure under (a) Planar Sliding, (b) Wedge Sliding and (c) Flexural Toppling for Change in Slope Dip Angle (Slope Code-SA6) 211

5.27 Graphs Showing Variation in Critical Percentage of Failure under (a) Planar Sliding, (b) Wedge Sliding and (c) Flexural Toppling for Change in Slope Dip Direction (Slope Code-SA6) 211

5.28 Graphs Showing Variation in Critical Percentage of Failure under (a) Planar Sliding, (b) Wedge Sliding and (c) Flexural Toppling for Change in Slope Dip Angle (Slope Code-SA7) 212

5.29 Graphs Showing Variation in Critical Percentage of Failure under (a) Planar Sliding, (b) Wedge Sliding and (c) Flexural Toppling for Change in Slope Dip Direction (Slope Code-SA7) 212

5.30 Graphs Showing Variation in Critical Percentage of Failure under (a) Planar Sliding, (b) Wedge Sliding and (c) Flexural Toppling for Change in Slope Dip Angle (Slope Code-SA8) 213

5.31 Graphs Showing Variation in Critical Percentage of Failure under (a) Planar Sliding, (b) Wedge Sliding and (c) Flexural Toppling for Change in Slope Dip Direction (Slope Code-SA8) 213

5.32 Graphs Showing Variation in Critical Percentage of Failure under (a) Planar Sliding, (b) Wedge Sliding and (c) Flexural Toppling for Change in Slope Dip Angle (Slope Code-SA9) 214

5.33 Graphs Showing Variation in Critical Percentage of Failure under (a) Planar Sliding, (b) Wedge Sliding and (c) Flexural Toppling for Change in Slope Dip Direction (Slope Code-SA10) 214

5.34 Graphs Showing Variation in Critical Percentage of Failure under (a) Planar Sliding, (b) Wedge Sliding and (c) Flexural Toppling for Change in Slope Dip Angle (Slope Code-SA1) 215

5.35 Graphs Showing Variation in Critical Percentage of Failure under (a) Planar Sliding, (b) Wedge Sliding and (c) Flexural Toppling for Change in Slope Dip Direction (Slope Code-SA1) 215

6.1 Locations of IMD and SASE Rain Gauges in Upper Beas Catchment 222

6.2 Algorithm for Creation of Gridded Rainfall Data at Micro Scale and Rainfall Analysis 224

6.3 Variation Plot for Mean Annual Rainfall in UBC using High Resolution Gridded Dataset ($0.625' \times 0.625'$) along North-South and East-West. 225

6.4 Comparison of Prepared Gridded Daily Rainfall Dataset at $0.625' \times 0.625'$ Scale with Existing Dataset at the$0.25^o \times 0.25^o$ Scale for Two Stations in UBC 226

6.5 Annual Maximum Rainfall (R_{max}) Isohyets Maps for $1^o \times 1^o$ Geographical Grid with the Spatial Resolution of $0.625' \times 0.625'$ for Years Before 1960 228

6.6 Annual Maximum Rainfall (R_{max}) Isohyets Maps for $1^o \times 1^o$ Geographical Grid with the Spatial Resolution of $0.625' \times 0.625'$ for Years After 1960 229

6.7 Annual Maximum Rainfall (R_{max}) Contour Maps for UBC with the Spatial Resolution of $0.625' \times 0.625'$ from Year 1901-1906 231

6.8 Annual Maximum Rainfall (R_{max}) Contour Maps for UBC with the Spatial Resolution of $0.625' \times 0.625'$ from Year 1907-19012 232

6.9 Annual Maximum Rainfall (R_{max}) Contour Maps for UBC with the Spatial Resolution of $0.625' \times 0.625'$ from Year 1913-1918 233

6.10 Annual Maximum Rainfall (R_{max}) Contour Maps for UBC with the Spatial Resolution of $0.625' \times 0.625'$ from Year 1919-1924 234

6.11 Annual Maximum Rainfall (R_{max}) Contour Maps for UBC with the Spatial Resolution of $0.625' \times 0.625'$ from Year 1925-1930 235

6.12 Annual Maximum Rainfall (R_{max}) Contour Maps for UBC with the Spatial Resolution of $0.625' \times 0.625'$ from Year 1931-1936 236

6.13 Annual Maximum Rainfall (R_{max}) Contour Maps for UBC with the Spatial Resolution of $0.625' \times 0.625'$ from Year 1937-1942 237

6.14 Annual Maximum Rainfall (R_{max}) Contour Maps for UBC with the Spatial Resolution of $0.625' \times 0.625'$ from Year 1943-1948 238

6.15 Annual Maximum Rainfall (R_{max}) Contour Maps for UBC with the Spatial Resolution of $0.625' \times 0.625'$ from Year 1949-1954 239

6.16 Annual Maximum Rainfall (R_{max}) Contour Maps for UBC with the Spatial Resolution of $0.625' \times 0.625'$ from Year 1955-1960 240

6.17 Annual Maximum Rainfall (R_{max}) Contour Maps for UBC with the Spatial Resolution of $0.625' \times 0.625'$ from Year 1961-1966 241

6.18 Annual Maximum Rainfall (R_{max}) Contour Maps for UBC with the Spatial Resolution of $0.625' \times 0.625'$ from Year 1967-1972 242

6.19 Annual Maximum Rainfall (R_{max}) Contour Maps for UBC with the Spatial Resolution of $0.625' \times 0.625'$ from Year 1973-1978 243

6.20 Annual Maximum Rainfall (R_{max}) Contour Maps for UBC with the Spatial Resolution of $0.625' \times 0.625'$ from Year 1979-1984 244

6.21 Annual Maximum Rainfall (R_{max}) Contour Maps for UBC with the Spatial Resolution of $0.625' \times 0.625'$ from Year 1985-1990 245

6.22 Annual Maximum Rainfall (R_{max}) Contour Maps for UBC with the Spatial Resolution of $0.625' \times 0.625'$ from Year 1991-1996 246

6.23 Annual Maximum Rainfall (R_{max}) Contour Maps for UBC with the Spatial Resolution of $0.625' \times 0.625'$ from Year 1997-2002 247

6.24 Annual Maximum Rainfall (R_{max}) Contour Maps for UBC with the Spatial Resolution of $0.625' \times 0.625'$ from Year 2003-2008 248

6.25 Annual Maximum Rainfall (R_{max}) Contour Maps for UBC with the Spatial Resolution of $0.625' \times 0.625'$ from Year 2009-2013 249

6.26 Total Monthly Rainfall Mean (R_{tm}) Isohyets Plots for $1^o \times 1^o$ Geographical Grid from January to June Over 1901-2013 252

6.27 Total Monthly Rainfall Mean (R_{tm}) Isohyets Plots for $1^o \times 1^o$ Geographical Grid from July to December Over 1901-2013 253

6.28 Trend of Total Monthly Rainfall Mean (R_{tm}) Over 1901-2013 254

6.29 Trend of Coefficient of Variation (CoV) (in %) for Slope SA/1-SA/10 256

6.30 1901-2013 Maximum Annual Rainfall Fluctuations for Slope SA/1 258

6.31 1901-2013 Maximum Annual Rainfall Fluctuations for Slope SA/2 258

6.32 1901-2013 Maximum Annual Rainfall Fluctuations for Slope SA/3 259

6.33 1901-2013 Maximum Annual Rainfall Fluctuations for Slope SA/4 259

6.34 1901-2013 Maximum Annual Rainfall Fluctuations for Slope SA/5 260

6.35 1901-2013 Maximum Annual Rainfall Fluctuations for Slope SA/6 260

6.36 1901-2013 Maximum Annual Rainfall Fluctuations for Slope SA/7 261

6.37 1901-2013 Maximum Annual Rainfall Fluctuations for Slope SA/8 261

6.38 1901-2013 Maximum Annual Rainfall Fluctuations for Slope SA/9 262

6.39 1901-2013 Maximum Annual Rainfall Fluctuations for Slope SA/10 262

6.40 Algorithm for Return Period and Frequency Analysis 263

6.41 Moment Ratios Diagrams Based on the Ordinary Moments 266

6.42 Comparison of Gumbel Distribution with Other Distribution Methods 266

6.43 Gumbel Distribution Plot for Slope SA/1 267

6.44 Gumbel Distribution Plot for Slope SA/2 267

6.45 Gumbel Distribution Plot for Slope SA/3 268

6.46 Gumbel Distribution Plot for Slope SA/4 268

6.47 Gumbel Distribution Plot for Slope SA/5 269

6.48 Gumbel Distribution Plot for Slope SA/6 269

6.49 Gumbel Distribution Plot for Slope SA/7 270

6.50 Gumbel Distribution Plot for Slope SA/8 270

6.51 Gumbel Distribution Plot for Slope SA/9 271

6.52 Gumbel Distribution Plot for Slope SA/10 271

7.1 Algorithm to Predisposing Parameters for Landslide Hazard 279

7.2 Slope Map of the Upper Beas Catchment 281

7.3 Aspect Map of the Upper Beas Catchment 283

7.4 Relative Relief Map of the Upper Beas Catchment 285

7.5 Land Use and Land Cover Map of the Upper Beas Catchment 288

7.6 Lithology and Geology Map of the Upper Beas Catchment 290

7.7 Seismo Tectonic Map of the Upper Beas Catchment 293

7.8 Fault Proximity Map of the Upper Beas Catchment 295

7.9 Road Proximity Map of the Upper Beas Catchment 297

7.10 Drainage Buffer Map of the Upper Beas Catchment 299

7.11 Drainage Density Map of the Upper Beas Catchment 301

7.12 Algorithm for Pre-processing Dataset and GIS Data Preparation 305

7.13 Algorithm for Preparation of Landslide Hazard Zonation Maps 312

7.14 Slope and Relative Relief Reclassified Factor Classes with their Representative Values 314

7.15 Geology and Road Proximity Reclassified Factor Classes with their Representative Values 315

7.16 Fault Buffer and Seismic Zones Factor Classes with their Representative Values 316

7.17 Land Use, Land Cover and Slope Aspect with their Representative Values 317

7.18 Stream Buffer and Stream Density Reclassified Factor Classes with their Representative Values 318

7.19 Algorithm for Rainfall Based Landslide Hazard Zonation 319

7.20 Rainfall Integrated Landslide Hazard Zonation Map for Return Period of 10 Years 323

7.21 Rainfall Integrated Landslide Hazard Zonation Map for Return Period of 20 Years 324

7.22 Rainfall Integrated Landslide Hazard Zonation Map for Return Period of 50 Years 325

7.23 Rainfall Integrated Landslide Hazard Zonation Map for Return Period of 100 Years 326

8.1 Algorithm for the Development of Numerical Model 333

8.2 3D Model Formulated for Slope SA/1 - SA/4 (Perspective and Top View) 334

8.3 3D Model Formulated for Slope SA/5 - SA/8 (Perspective and Top View) 335

8.4 3D Model Formulated for Slope SA/9 and SA/10 (Perspective and Top View) 336

8.5 Extremely Fine Meshing for Slope SA/1 - SA/10 338

8.6 Hydro-mechanical Boundaries for Slope Model 339

8.7 Material Parameters used in Hydro-mechanical Model 342

8.8 Geological Strength Index as Estimates from the Field Observations for the Slopes (SA/1 - SA/10) 343

8.9 Hydro-mechanical Model and its Components 344

8.10 Variation between Annual Maximum Rainfall and Annual Minimum Factor of Safety for Slope SA/1 over 113 Years 347

8.11 Variation between Annual Maximum Rainfall and Annual Minimum Factor of Safety for Slope SA/2 over 113 Years 347

8.12 Variation between Annual Maximum Rainfall and Annual Minimum Factor of Safety for Slope SA/3 over 113 Years 348

8.13 Variation between Annual Maximum Rainfall and Annual Minimum Factor of Safety for Slope SA/4 over 113 Years 348

8.14 Variation between Annual Maximum Rainfall and Annual Minimum Factor of Safety for Slope SA/5 over 113 Years 349

8.15 Variation between Annual Maximum Rainfall and Annual Minimum Factor of Safety for Slope SA/6 over 113 Years 349

8.16 Variation between Annual Maximum Rainfall and Annual Minimum Factor of Safety for Slope SA/7 over 113 Years 350

8.17 Variation between Annual Maximum Rainfall and Annual Minimum Factor of Safety for Slope SA/8 over 113 Years 350

8.18 Variation between Annual Maximum Rainfall and Annual Minimum Factor of Safety for Slope SA/9 over 113 Years 351

8.19 Variation between Annual Maximum Rainfall and Annual Minimum Factor of Safety for Slope SA/10 over 113 Years 351

8.20 Slope Model Showing Pressure Contours as Developed under Rainfall for Year 1901 in Slope SA/1 353

8.21 Variation Between Annual Maximum Rainfall and Pore Water Pressure (Top & Bottom) for Slope SA/1 over 113 Years 354

8.22 Variation Between Annual Maximum Rainfall and Pore Water Pressure (Top & Bottom) for Slope SA/2 over 113 Years 354

8.23 Variation Between Annual Maximum Rainfall and Pore Water Pressure (Top & Bottom) for Slope SA/3 over 113 Years 355

8.24 Variation Between Annual Maximum Rainfall and Pore Water Pressure (Top & Bottom) for Slope SA/4 over 113 Years 355

8.25 Variation Between Annual Maximum Rainfall and Pore Water Pressure (Top & Bottom) for Slope SA/5 over 113 Years 356

8.26 Variation Between Annual Maximum Rainfall and Pore Water Pressure (Top & Bottom) for Slope SA/6 over 113 Years 356

8.27 Variation Between Annual Maximum Rainfall and Pore Water Pressure (Top & Bottom) for Slope SA/7 over 113 Years 357

8.28 Variation Between Annual Maximum Rainfall and Pore Water Pressure (Top & Bottom) for Slope SA/8 over 113 Years 357

8.29 Variation Between Annual Maximum Rainfall and Pore Water Pressure (Top & Bottom) for Slope SA/9 over 113 Years 358

8.30 Variation Between Annual Maximum Rainfall and Pore Water Pressure (Top & Bottom) for Slope SA/10 over 113 Years 358

8.31 Variation between Annual Maximum Rainfall and Total Displacement (Top & Bottom) for Slope SA/1 over 113 years 361

8.32 Variation between Annual Maximum Rainfall and Total Displacement (Top & Bottom) for Slope SA/2 over 113 Years 361

8.33 Variation between Annual Maximum Rainfall and Total Displacement (Top & Bottom) for Slope SA/3 over 113 Years 362

8.34 Variation between Annual Maximum Rainfall and Total Displacement (Top & Bottom) for Slope SA/4 over 113 Years 362

8.35 Variation between Annual Maximum Rainfall and Total Displacement (Top & Bottom) for Slope SA/5 over 113 Years 363

8.36 Variation between Annual Maximum Rainfall and Total Displacement (Top & Bottom) for Slope SA/6 over 113 Years 363

8.37 Variation between Annual Maximum Rainfall and Total Displacement (Top & Bottom) for Slope SA/7 over 113 Years 364

8.38 Variation between Annual Maximum Rainfall and Total Displacement (Top & Bottom) for Slope SA/8 over 113 Years 364

8.39 Variation between Annual Maximum Rainfall and Total Displacement (Top & Bottom) for Slope SA/9 over 113 Years 365

8.40 Variation between Annual Maximum Rainfall and Total Displacement (Top & Bottom) for Slope SA/10 over 113 Years 365

8.41 Saturation Iso-surfaces for Slope SA/4 366

8.42 Variation between Annual Maximum Rainfall and Degree of Saturation (Top & Bottom) for Slope SA/1 over 113 Years 367

8.43 Variation between Annual Maximum Rainfall and Degree of Saturation (Top & Bottom) for Slope SA/2 over 113 Years 367

8.44 Variation between Annual Maximum Rainfall and Degree of Saturation (Top & Bottom) for Slope SA/3 over 113 Years 368

8.45 Variation between Annual Maximum Rainfall and Degree of Saturation (Top & Bottom) for Slope SA/4 over 113 Years 368

8.46 Variation between Annual Maximum Rainfall and Degree of Saturation (Top & Bottom) for Slope SA/5 over 113 Years 369

8.47 Variation between Annual Maximum Rainfall and Degree of Saturation (Top & Bottom) for Slope SA/6 over 113 Years 369

8.48 Variation between Annual Maximum Rainfall and Degree of Saturation (Top & Bottom) for Slope SA/7 over 113 Years 370

8.49 Variation between Annual Maximum Rainfall and Degree of Saturation (Top & Bottom) for Slope SA/8 over 113 Years 370

8.50 Variation between Annual Maximum Rainfall and Degree of Saturation (Top & Bottom) for Slope SA/9 over 113 Years 371

8.51 Variation between Annual Maximum Rainfall and Degree of Saturation (Top & Bottom) for Slope SA/10 over 113 Years 371

E.1 Landslide Location L-2 553
E.2 Landslide Location L-5 554
E.3 Landslide Location L-6 554
E.4 Landslide Location L-7 555
E.5 Landslide Location L-9 555
E.6 Landslide Location L-10 556
E.7 Landslide Location L-11 556
E.8 Landslide Location L-14 557
E.9 Landslide Location L-16 557
E.10 Landslide Location L-18 558
E.11 Landslide Location L-21 558

List of Tables

1.1 Top Five Countries with Rainfall Induced Landslides and the Total Number of People Affected (source EM-DAT-2018). 2

1.2 Indian Scenario of Landslide Affected People and Total Property Loss 1950-2017 (Source EM-DAT-2018) 3

1.3 Most Recent Cloudbursts and Resulting Landslides in the Upper Beas Catchment and its Vicinity, Himachal Pradesh 5

2.1 Landslide Classification based on Type of Movement, Material Involved and the Velocity Classes (updated from Cruden and Varnes (1996)) Classification 21

2.2 Four Major Landslide Controlling Process and their Causative Factors (Cruden and Varnes, 1996; Wyllie and Mah, 2004) 23

3.1 Reported Landslides in Upper Beas Catchment (2012-Data DDMA) 76

3.2 Stratigraphic Sequence of the Upper Beas Catchment (Raj and Singh, 1989; Kumbkarni, 2000; Sharma, 2002) 91

3.3 Major Geomorphic Units in Himachal Himalayas (Bhambri et al., 1995) 97

3.4 Mean Monthly Rainfall (mm) for IMD station at District Kullu and Lahaul & Spiti 114

3.5 Last 100 Years (1915-2016) Annual Mean of Minimum, Average and Maximum Temperature (in ^oC) for IMD Station at Kullu and Lahaul & Spiti 115

3.6 Landslide Size Distribution Identified through Remote Sensing Studies; and Number of Landslide Considered for Field Survey and this Study 117

3.7 Locations of Visited Landslide (L01 - L21) and Locations Selected for Detailed Study (SA/1 - SA/10) for the Upper Beas Catchment 120

3.8 Slope Variables Considered for Primary Slope Quality Assessment 125

3.9 Slope Variables Considered for Deterministic Slope Assessment 126

3.10 Description of Joint Parameters (IS-11315, 1987) and Estimation of Rock Mass Rating (Bieniawski, 1989) for Selected Landslide Locations 128

3.11 Description of Joint Parameters (IS-11315, 1987) and Estimation of Rock Mass Rating (Bieniawski, 1989) for Selected Landslide Locations 129

4.1 Major Crystalline Phases Detected in XRD Analyses 147

4.2 XRD Weight Percentage of Phyllitic-quartzite, Quartzitic-phyllite and Migmatitic-gneiss 147

4.3 Physical Properties of Rock Specimens 157

4.4 Slake Durability Test Results 159

4.5 Brazilian Tensile Strength (σ_t) at $\beta = 0^o$ 160

4.6 Brazilian Tensile Strength (σ_t) Values at Various β Angle 161

4.7 Uniaxial Compression Strength, Poisson's Ratio and Modulus of Elasticity for Rock Specimens 165

4.8 Compressive Strength of Rock Specimens at Various Confining Pressure 168

4.9 Shear Strength Parameters for Phyllitic-quartzite, Quartzitic-phyllite and Migmatitic-gneiss 171

4.10 Percentage Decrement upon Saturation for Phyllitic-quartzite, Quartzitic-phyllite and Migmatitic-gneiss 171

4.11 Shear strength Parameters Along the Foliation Plane Obtained under Oblique Shear Testing 176

4.12 Permeability of Rock Specimens 177

4.13 Variation in Permeability Values of Phyllitic-quartzite, Quartzitic-phyllite and Migmatitic-gneiss Rock Specimens 180

5.1 Selected Landslides for Kinematic Analysis 185

5.2 Dominating Joint Sets (Dip Direction/Amount) for Landslide Locations 191

5.3 Unidirectional Increment in Critical Percentage of Planar, Wedge and Toppling Failures upon Saturation 203

6.1 Total Monthly Rainfall (in mm) for Slopes, Averaged Over 1901-2013 255

6.2 Coefficient of Variation (CoV) (in %) for Slopes, Averaged Over 1901-2013 255

6.3 Ranking of Candidate Distributions Based on AIC and BIC 265

6.4 Rainfall (in mm) Return Period $R_{(p)}$ (in Years) for all Slopes 272

7.1 Data Sets and Sources 277

7.2 Slope Angle of Upper Beas Catchment and the Total Area Covered 282

7.3 Aspect of the Upper Beas Catchment and Total Area Covered 284

7.4 Relative Relief of the Upper Beas Catchment and Total Area covered 286

7.5 Land Use and Land Cover of the Upper Beas Catchment and Total Area Covered 287

7.6 Lithology and Stratigraphic Units of the Upper Beas Catchment and the Total Area Covered 291

7.7 Earthquake Zones of the Upper Beas Catchment and Total Area Covered 292

7.8 Proximity to Major Faults in the Upper Beas Catchment and the Total Area Covered 294

7.9 Proximity to Major Roads in the Upper Beas Catchment and the Total Area Covered 296

7.10 Proximity to Streams (Drainage Buffer) in the Upper Beas Catchment and the Total Area Covered 298

7.11 Drainage Desity of the Upper Beas Catchment and the Total Area Covered 300

7.12 Slope Angle and Relative Relief Reclassified Factor Classes and their Representative Values 308

7.13 Geology/Lithology Reclassified Factor Classes and their Representative Values 308

7.14 Proximity Reclassified Factor Classes and their Representative Values 309

7.15 Land-Use, Land-Cover and Land-Capability Reclassified Factor Classes and their Representative Values 309

7.16 River/Stream and Lineament Density Reclassified Factor Classes and their Representative Values 309

7.17 Individual Factors Weightage and Respective Classes Ratings for Landslide Hazard Analysis 310

7.18 Rainfall Return Period Weightage and Respective Classes Ratings for Rainfall Based Landslide Hazard Analysis 322

7.19 Area under Various Landslide Hazard Zones for the Return Period of 10, 20, 50 and 100 Years 327

8.1 Model Dimensions and the Slope Heights 336

8.2 Physical and Mechanical Properties of Rocks 341

8.3 Geological Strength Index Values, Disturbance Factor and Hoek-Brown Parameters for Slopes under Dry and Saturated Conditions 344

8.4 Minimum and Maximum FOS Obtained at Maximum and Minimum Rainfall over 113 Years 346

8.5 Rainfall Return Period (R_P) and their Respective Factor of Safety 346

8.6 Maximum and Minimum (Limits) of Pore Water Pressure at Top and Bottom of Slopes 353

8.7 Maximum and Minimum Displacement With Respect to Rainfall at the Crown and Toe of Slopes 359

8.8 Total Cumulative Displacement of the Toe and Crown of Slopes 360

A.1 Landslide Inventory of India from 1948 to 2017 411

B.1 Landslide Locations Recorded by Remote Sensing Studies and Field Investigation 425

B.2 Annual Maximum Rainfall Data as Obtained from HRGRD Analysis for Slope SA/1 to SA/10 428

B.3 Total Monthly Rainfall Data as Obtained from HRGRD Analysis for Slope SA/1 to SA/10 from 1901 (-01) to 2013 (-13) 431

C.1 Result of Sensitivity Analysis for Slope SA/1 with Continuous Change in Slope Dip Amount (Angle) 477

C.2 Result of Sensitivity Analysis for Slope SA/1 with Continuous Change in Slope Dip Direction 480

C.3 Recorded Dip Amount (DA) and Direction (DD) Data (in Degrees) for Kinematic Analysis of Slopes (SA/1 - SA/10) 492

D.1 Numerical Analysis Results for Slope SA/1 as Plotted in Chapter 8 513

D.2 Numerical Analysis Results for Slope SA/2 as Plotted in Chapter 8 517

D.3 Numerical Analysis Results for Slope SA/3 as Plotted in Chapter 8 521

D.4 Numerical Analysis Results for Slope SA/4 as Plotted in Chapter 8 525

D.5 Numerical Analysis Results for Slope SA/5 as Plotted in Chapter 8 529

D.6 Numerical Analysis Results for Slope SA/6 as Plotted in Chapter 8 533

D.7 Numerical Analysis Results for Slope SA/7 as Plotted in Chapter 8 537

D.8 Numerical Analysis Results for Slope SA/8 as Plotted in Chapter 8 541

D.9 Numerical Analysis Results for Slope SA/9 as Plotted in Chapter 8 545

D.10 Numerical Analysis Results for Slope SA/10 as Plotted in Chapter 8 549

List of Abbreviations

The following list defines the principle Abbreviations and their definitions as used in the thesis. Abbreviations not listed here are defined as they appear in the text.

CPS	Counts per Second
ICDD	International Centre for Diffraction Data
COD	Crystallography Open Database
XRD	X-Ray Powder diffraction
PDF	Powder Diffraction File
SEM	Scanning Electron Microscopy
PQ	Phyllitic-quartzite
QP	Quartzitic-phyllite
MG	Migmatitic-gneiss
L/D	Length/Diameter
IS	Indian Standards
ASTM	American Society for Testing and Materials
SDI	Slack Durability Index
NBSS-LUP	National Bureau of Soil Survey and Land Use Planning
APHRODITE	Asian Precipitation-Highly Resolved Observational Data Integration Towards Evaluation of the Water Resources
ISRM	International Society for Rock Mechanics
UCS	Uniaxial Compressive Strength
SFS	Single Faced Slope
MFS	Multiple Faced Slope
FOS	Factor of Safety
UBC	Upper Beas Catchment
RQD	Rock Quality Designation

SRA	Slope Response Analysis
NDC	National Data Center
IMD	India Meteorological Department
MSM	Modified Shepard's Method
HRGD	High Resolution Gridded Data
SASE	Snow and Avalanche Study Establishment
IDW	Inverse Distance Weighing
CoV	Coefficient of Variation
LPIII	Log-Pearson Type III
PPCC	Probability Plot Correlation Coefficient
MEF	Mean Excess Function
HA	Halphen Type A
HB	Halphen Type B
HIB	Halphen Type IB
GEV	Generalized Extreme Value
EV1	Extreme Value 1
GPA	Grade Point Average
LOGN	Log Normal
GPAR	Generalized Pareto Average Relation
IG	Inverse Gamma
LN	Log Normal
MMR	Mean Monthly Rainfall
AR	Annual Rainfall
AIC	Akaike's Information Criterion
BIC	Bayesian Information Criterion
IFRC	International Federation of Red Cross and Red Crescent Societies
CRED	Centre for Research on the Epidemiology of Disasters
LHZ	Landslide Hazard Zonation

LSZ	Landslide Susceptibility Zonation
GIS	Geographic Information System
SoI	Survey of India
DEM	Digital Elevation Model
GSI	Geological Survey of India
LU-LC	Land Use and Land Cover
LI	Landslide Inventory
RS	Remote Sensing
MSL	Mean Sea Level
BIS	Bureau of Indian Standards
MCT	Main Central thrust
WGS	World Geodetic System
UTM	Universal Transverse Mercator
FLAASH	Fast Line-of-sight Atmospheric Analysis of Spectral Hypercubes
FCCs	False Colour Composites
NDVI	Normalized Difference Vegetation Index
NIR	Near Infrared
AHP	Analytical Hierarchy Process
WLC	Weighted Linear Combination
MCE	Multicriteria Evaluation
InfoVal	Information Value
VHH	Very High Hazard
HH	High Hazard
MH	Medium Hazard
LH	Low Hazard
VLH	Very Low Hazard
LNRF	Landslide Nominal Risk Factor
LFA	Landslide Frequency Analysis

MHA	Multivariate Heuristic Approach
HM	Hydromechanical
PWP	Pore Water Pressure

List of Notations

The following list defines the principle symbols and their berief definition as used in the thesis. Symbols not listed here are defined as they appear in the text.

θ	Angle in radians
μm	Distance in micrometers
$^{\circ}C$	Degree Celcius (Temperature Unit)
α	Wavelength
β	Beta Particle Emission
$\dot{A}$	Ångström
mm, cm, m	Length S.I. units as millimeters, centimeters and meters
mA	milliamperes (Current Unit)
kV	kilovolts (Voltage unit)
γ_{dry}	Dry unit weight
M_D	Dry mass
Kg, g	Weight S.I. units as kilograms and grams
γ_{sat}	Saturated unit weight
ρ_{dry}	Dry density
ρ_{sat}	Saturated density
η	Porosity
V_v	Volume of Voids
M_S	Saturated mass
hr, min, s	Time S.I unit as hours, minutes and seconds
σ_t	Ultimate Tensile Strength
$\sigma_{t(dry)}$	Dry Tensile Strength
$\sigma_{t(sat)}$	Saturated Tensile Strength
σ	Normal Stress

φ	Lamination Orientation
σ_c	Uniaxial Compressive Strength
Ω	Ohms (Resistance Unit)
$^\circ F$	degree Fahrenheit (Temperature Unit)
E	Modulus of Elasticity
ν	Poisson's Ratio
E_{T50}	Tangent Young's modulus at 50% Ultimate Strength
ϕ	Angle of Shear Resistance or the Angle of Internal Friction
c	Cohesion
σ_1	Major Principal Stress
σ_2	Intermediate Principal Stress
σ_3	Minor Principal Stress
MPa, KPa	Pressure S.I. unit as Megapascals and Kilopascals
psi	Pressure Imperial unit as pound per second
m_s	Gradient or Slope
b	Intercept on y-axis
τ	Shear Stress
σ_n	Normal Stress
k	Coefficient of Hydraulic Conductivity or Permeability
J_v	Volumetric Joint Count
S	Joint Spacing
J_n	Joint Set Number
m^3	Volume in cubic metres
i	Roughness Angle
R	Rebound Values
θ_t	Tilt Angle
λ	Trend of the Line
φ	Plunge of the Line

δ	Dip Direction
ψ	Dip Amount
W_{cf}	Critical Percentage of Wedge Failure
P_{cf}	Critical Percentage of Planer Failure
T_{cf}	Critical Percentage of Toppling Failure
R_{max}	Annual Maximum Rainfall
R_{tm}	Total Monthly Rainfall Mean
γ_{mG}	Modified Gumbel Variate
$R_{(p)}$	Return Period in Years
km^2	Area in square kilometres
km	Distance in kilometres
D_d	Drainage Density
RV	Representative Values
P_f	Interstitial Pressure
F_n	Factor of Safety corresponding to n Years Return Period
R_{min}	Annual Minimum Rainfall
F_{max}	Factor of Safety corresponding to R_{max}
F_{min}	Factor of Safety corresponding to R_{min}
PWP_{tmax}	Pore Water Pressure at Top corresponding to R_{max}
PWP_{tmin}	Pore Water Pressure at Top corresponding to R_{min}
PWP_{bmax}	Pore Water Pressure at Base corresponding to R_{max}
PWP_{bmin}	Pore Water Pressure at Base corresponding to R_{min}
D_{max}	Displacement corresponding to R_{max}
D_{min}	Displacement corresponding to R_{min}
D_{crown}	Displacement at Crown
D_{toe}	Displacement at Toe